PHYSICAL REVIEW B **83**, 041404(R) (2011)

Seebeck coefficients in nanoscale junctions: Effects of electron-vibration scattering and local heating

Bailey C. Hsu,[1] Yu-Shen Liu,[1,4] Sheng Hsien Lin,[2,3] and Yu-Chang Chen[1,*]

[1]*Department of Electrophysics, National Chiao Tung University, 1001 Ta Hsueh Road, Hsinchu 30010, Taiwan*

[2]*Department of Applied Chemistry, National Chiao Tung University, 1001 Ta Hsueh Road, Hsinchu 30010, Taiwan*

[3]*Institute of Atomic and Molecular Sciences, Academia Sinica, Taipei 106, Taiwan*

[4]*College of Physics and Engineering, Changshu Institute of Technology, Suzhou 215500, China*

(Received 29 September 2010; revised manuscript received 16 December 2010; published 25 January 2011)

We report first-principles calculations of inelastic Seebeck coefficients in an aluminum monatomic junction. We compare the elastic and inelastic Seebeck coefficients with and without local heating. In the low-temperature regime, the signature of normal modes in the profiles of the inelastic Seebeck effects is salient. The inelastic Seebeck effects are enhanced by the normal modes and further magnified by local heating. In the high-temperature regime, the inelastic Seebeck effects are weakly suppressed due to the quasiballistic transport.

DOI: 10.1103/PhysRevB.83.041404 PACS number(s): 73.63.Nm, 71.15.Mb, 73.63.Rt

The electron-vibration interaction plays an important role in molecular electronics. Electrons flowing in nanojunctions are characterized by quasiballistic electron transport.[1] Only a small fraction of electrons experience the inelastic scattering. Electron-vibration interactions cause discontinuities in the current-voltage (I-V) characteristics known as inelastic current tunneling spectroscopy (IETS).[2] IETS can provide information on the underlying atomic structures of junctions.[3] It also gives important signals to the molecular junction characterization.[4]

Electrons that travel with energies larger than the energy of normal modes can excite corresponding vibrations in the nanostructure anchoring the electrodes. This effect causes local heating in the nanostructure.[5–7] Heating occurs when electrons exchange energy with the excitation and relaxation of the energy levels of the vibration of the nanostructured object that anchors the electrodes. The heating power is typically within 10% of the electric power (IV_B) supplied by a battery even at ambient temperatures because of quasiballistic transport. The heat generated in the central wire region is dissipated to the bulk electrodes via phonon-phonon interactions. The heat generation eventually equilibrates the heat dissipation, where the wire region reaches an effective local temperature T_w higher than the electrode temperature T_e. Local temperature depends on several factors: the strength of coupling between electrons and the vibrations, the background temperature, and the thermal current which dissipates heat.

In the past decade, remarkable progress has been achieved in measuring the Seebeck coefficients in nanojunctions.[8,9] These experiments have shed light on the design of possible energy-conversion nanodevices, such as nanoscale refrigerators and power generators.[10] These experiments have also inspired rapid development in the theory of thermoelectric nanojunctions.[11–20] In bulk systems, diffused electrons scattered by phonons can significantly affect the Seebeck coefficient. However, the effects of the quasiballistic electrons scattered by vibrations of the nanostructure on the Seebeck coefficient are relatively unexplored in nanojunctions.[21,22] The Seebeck coefficient is usually defined under no current in the literature. In this paper, we investigate inelastic Seebeck coefficients under external biases from first-principles approaches. This may offer new possibilities of engineering systems where nonequilibrium current and inelastic effects would enhance the thermopower.[23]

The many-body Hamiltonian of the system under consideration is $H = H_{\rm el} + H_{\rm vib} + H_{\text{el-vib}}$,[5] where $H_{\rm el}$ is the electronic part of the Hamiltonian under adiabatic approximations and $H_{\rm vib}$ is the ionic part of the Hamiltonian, which can be cast into a set of independent simple harmonic oscillators via normal coordinates. The normal-mode frequencies are ω_j, and $H_{\text{el-vib}}$ is a part of the Hamiltonian for electron-vibration interactions which has the form of

$$H_{el\text{-}vib} = \sum_{\alpha,\beta,E_1,E_2,j} \left(\sum_{i,\mu} \sqrt{\frac{\hbar}{2M_i\omega_j}} A_{i\mu,j} J^{i\mu,\alpha\beta}_{E_1,E_2} \right) \times a^{\alpha\dagger}_{E_1} a^{\beta}_{E_2} (b_j + b^{\dagger}_j), \tag{1}$$

where $\alpha,\beta = \{L,R\}$; M_i is the mass of the ith atom; $A_{i\mu,j}$ is a canonical transformation between normal and Cartesian coordinates satisfying $\sum_{i,\mu} A_{i\mu,j} A_{i\mu,j'} = \delta_{j,j'}$; b_j is the annihilation operator corresponding to the jth normal mode, and $a^{L(R)}$ is the annihilation operator for electrons; the coupling constant $J^{i\mu,\alpha\beta}_{E_1,E_2}$ between electrons and the vibration of the ith atom in μ $(= x, y, z)$ component can be calculated as

$$J^{i\mu,\alpha\beta}_{E_1,E_2} = \int d\mathbf{r} \int d\mathbf{K}_{\parallel} [\Psi^{\alpha}_{E_1\mathbf{K}_{\parallel}}(\mathbf{r})]^* [\partial_{\mu} V^{ps}(\mathbf{r},\mathbf{R}_i) \Psi^{\beta}_{E_2\mathbf{K}_{\parallel}}(\mathbf{r})], \tag{2}$$

where $V^{ps}(\mathbf{r},\mathbf{R}_i)$ is the pseudopotential representing the interaction between electrons and the ith ion; $\Psi^{\alpha(=L,R)}_{E\mathbf{K}_{\parallel}}(\mathbf{r})$ stands for the effective single-particle wave function of the entire system corresponding to incident electrons propagated from the left (right) electrode. These wave functions are calculated iteratively until convergence and self-consistency are achieved in the framework of DFT combined with the Lippmann-Schwinger equation,[24]

$$\Psi^{\alpha}_{E\mathbf{K}_{\parallel}}(\mathbf{r}) = \Psi^{\alpha}_{0,E\mathbf{K}_{\parallel}}(\mathbf{r}) + \int d\mathbf{r}_1 \int d\mathbf{r}_2 G(\mathbf{r},\mathbf{r}_1) V(\mathbf{r}_1,\mathbf{r}_2) \Psi^{\alpha}_{E\mathbf{K}_{\parallel}}(\mathbf{r}),$$

where G is the Green's function of the biased bimetallic electrodes with $V_B = (\mu_R - \mu_L)/e$, where $\mu_{R(L)}$ is the chemical potentials deep in the right (left) electrode, respectively;

the wave function of the bimetallic junction, $\Psi^{\alpha}_{0,E\mathbf{K}_{\parallel}}(\mathbf{r})$, is calculated by solving a combination of the Poisson and Schrödinger equations until self-consistency is achieved, where the boundary conditions are given by the electrons deep inside the biased electrodes. The inclusion of a single molecule bridging the bimetallic electrodes is considered as the scattering center, described by the potential V.

Our starting point is the inelastic current when considering electron-vibration interactions,

$$I(\mu_L,T_L;\mu_R,T_R;T_w) = \frac{2e}{h}\int dE\big[\big(f_E^R - f_E^L\big) - (\tilde{B}^R - \tilde{B}^L)\big]\tau(E), \quad (3)$$

where $f_E^{L(R)} = 1/\{\exp[(E-\mu_{L(R)})/(k_B T_{L(R)})]+1\}$ is the Fermi-Dirac distribution function describing the statistic of electrons deep in the left (right) electrode with temperature $T_{L(R)}$ and chemical potential $\mu_{L(R)}$; the transmission function $\tau(E) = \frac{\pi\hbar^2}{mi}\int d\mathbf{R}\int d\mathbf{K}_{||}(\Psi^{R*}_{EK_{\parallel}}\nabla\Psi^{R}_{EK_{\parallel}} - \nabla\Psi^{R*}_{EK_{\parallel}}\Psi^{R}_{EK_{\parallel}})$ is calculated from the electronic part of the wave functions $\Psi^{R}_{EK_{\parallel}}$. The terms $\tilde{B}^{L(R)}$ represent the corrections to the elastic current considering the eight first-order scattering processes depicted in Fig. 1,

$$\tilde{B}^{\alpha} = \sum_j \big[\big\langle\big|B^{\beta,\alpha}_{j,k}\big|^2\big\rangle f^{\alpha}_E\big(1-f^{\beta}_{E\pm\hbar\omega_j}\big) - \big\langle\big|B^{\alpha\alpha}_{j,k}\big|^2\big\rangle f^{\alpha}_E\big(1-f^{\alpha}_{E\pm\hbar\omega_j}\big)\big], \quad (4)$$

where $\alpha,\beta = \{L,R\}$ and $\alpha\neq\beta$. The parameters $B^{RR}_{j,1(2)}$ and $B^{LR}_{j,1(2)}$ denoted in Eq. (4) are

$$B^{\alpha R}_{j,1(2)} = i\pi\sum_{i\mu}\sqrt{\frac{\hbar}{2\omega_j}}A_{i\mu,j}J^{i\mu,\alpha R}_{E\pm\hbar\omega_j,E}D^{\alpha}_{E\pm\hbar\omega_j}\sqrt{\delta+\langle n_j\rangle}, \quad (5)$$

where $\alpha = \{L,R\}$; $\delta = 0(1)$ represents the process of phonon emission (absorption). The other two parameters in Eq. (4) can be obtained by the relations $B^{LL}_{j,1(2)} = -B^{RR}_{j,1(2)}$ and $B^{RL}_{j,1(2)} = -B^{LR}_{j,1(2)}$; the average number of local phonons is $\langle n_j\rangle = 1/\{\exp[\hbar\omega_j/(k_B T_w)]-1\}$, where T_w is the effective wire temperature.

The rate of energy absorbed (emitted) by the anchored nanostructures due to incident electrons from the $\beta=\{L,R\}$ electrode and scattered to the $\alpha=\{L,R\}$ electrode via a vibrational mode j is denoted by $W^{\alpha\beta,2(1)}_j$. The total thermal power generated in the junction P can be written as the sum of all the vibrational modes of eight scattering processes shown in Fig. 1,

$$P = \sum_{j\in\text{vib}}\sum_{\alpha=\{L,R\}}\sum_{\beta=\{L,R\}}\big(W^{\alpha\beta,2}_j - W^{\alpha\beta,1}_j\big), \quad (6)$$

where $W^{\alpha\beta,k}_j$ are calculated from the Fermi golden rule,

$$W^{\alpha\beta,k}_j = 2\pi\hbar(\delta_{k,2}+\langle n_j\rangle)\int dE\left|\sum_{i,\mu}A_{i\mu,j}J^{i\mu,\alpha\beta}_{E\pm\hbar\omega_j,E}\right|^2 \times f_E(\mu_\alpha,T_\alpha)[1-f_{E\pm\hbar\omega_j}(\mu_\beta,T_\beta)]D^{\alpha}_{E\pm\hbar\omega_j}D^{\beta}_{E}, \quad (7)$$

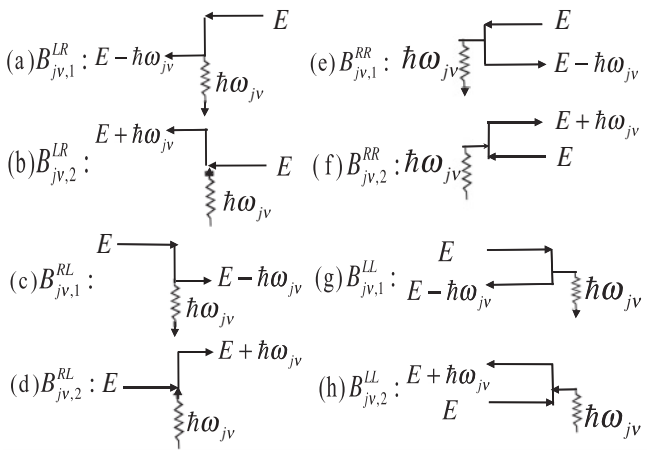

FIG. 1. Feynman diagrams of the first-order electron-vibration scattering processes considered in this study.

where $\alpha,\beta=\{L,R\}$ and $\delta_{k,2}$ is the Kronecker δ and $k=1$ (2) corresponding to relaxation (excitation) of the vibrational modes; D^{α} is partial density of states.

The rate of heat dissipated to electrodes via phonon-phonon interactions is calculated using the weak link model,[25]

$$J_{ph} = \frac{2\pi K^2}{\hbar}\int_0^{\infty} dE E N_L(E)N_R(E)[n_L(E)-n_R(E)], \quad (8)$$

where $K = 1.59\ \text{eV}/a_0^2$ is the stiffness of the 4-Al atom chain connected to the electrodes obtained from the total energy calculation,[26] $N_{L(R)}(E)$ is the spectral density of local phonon DOS at the left (right) electrode surface from first-principles calculations,[27] and $n_{L(R)} \equiv 1/(e^{E/K_B T_{L(R)}}-1)$ is the Bose-Einstein distribution function. The effective local temperature T_w is obtained when heat generation in the nanostructure and heat dissipation into the bulk electrodes reach balance.

We calculate the inelastic Seebeck coefficient based on the inelastic current described in Eq. (3) which is a function of T_L, T_R, T_w, and $V_B = (\mu_R-\mu_L)/e$. We consider an extra current induced by an infinitesimal temperature difference (ΔT) across the junction. This current is counterbalanced by an extra current driven by a voltage (ΔV), which is induced by ΔT via the Seebeck effect; that is,

$$I(\mu_L,T_L;\mu_R,T_R) = \left[I\left(\mu_L,T_L-\frac{\Delta T}{2};\mu_R,T_R+\frac{\Delta T}{2}\right) + I\left(\mu_L-\frac{e\Delta V}{2},T_L;\mu_R+\frac{e\Delta V}{2},T_R\right)\right]\Big/2. \quad (9)$$

After expanding the above equation to the first order in ΔT and ΔV, we obtain the inelastic Seebeck coefficient (defined as $S_{el+vib} = \Delta V/\Delta T$),

$$S_{\text{el+vib}} = -\frac{1}{e}\frac{\int dE\left(\frac{\partial\tilde{f}^R_E}{\partial T_R}+\frac{\partial\tilde{f}^L_E}{\partial T_L}\right)\tau(E)}{\int dE\left(\frac{\partial\tilde{f}^R_E}{\partial E}+\frac{\partial\tilde{f}^L_E}{\partial E}\right)\tau(E)}, \quad (10)$$

where

$$\frac{\partial \tilde{f}_E^\alpha}{\partial E} = \frac{\partial f_E^\alpha}{\partial E} - \sum_{j\in \text{vib};k=1,2} \left(C_{\mu,j,k}^{R\alpha} + C_{\mu,j,k}^{L\alpha}\right), \quad (11)$$

$$\frac{\partial \tilde{f}_E^\alpha}{\partial T_R} = \frac{\partial f_E^\alpha}{\partial T_R} - \sum_{j\in \text{vib};k=1,2} \left(C_{T,j,k}^{R\alpha} + C_{T,j,k}^{L\alpha}\right), \quad (12)$$

where $\alpha = \{L,R\}$ and the parameters $C_{\mu,j,1(2)}^{\alpha R}$ and $C_{T,j,1(2)}^{\alpha R}$ are

$$C_{\mu,j,1(2)}^{\alpha R} = \left[f_E^R \frac{\partial f_{E\pm\hbar\omega_{jv}}^\alpha}{\partial E} - \left(1 - f_{E\pm\hbar\omega_j}^\alpha\right) \frac{\partial f_E^R}{\partial E} \right] \left\langle \left| B_{j,1(2)}^{RR} \right|^2 \right\rangle, \quad (13)$$

$$C_{T,j,1(2)}^{\alpha R} = \left[\frac{E \pm \hbar\omega_j - \mu_\alpha}{T_R} f_E^R \frac{\partial f_{E\pm\hbar\omega_j}^\alpha}{\partial E} - \frac{E-\mu_R}{T_R} \left(1 - f_{E\pm\hbar\omega_j}^\alpha\right) \frac{\partial f_E^R}{\partial E} \right] \left\langle \left| B_{j,1(2)}^{\alpha R} \right|^2 \right\rangle, \quad (14)$$

where $\alpha = \{L,R\}$ and $B_{j,1(2)}^{\alpha\beta}$ are given by. Eq. (5). The other two terms in Eq. (10) can be calculated with the following relations $\frac{\partial \tilde{f}_E^L}{\partial T} = \frac{\partial \tilde{f}_E^R}{\partial T}(L \rightleftharpoons R)$ and $\frac{\partial \tilde{f}_E^L}{\partial E} = \frac{\partial \tilde{f}_E^R}{\partial E}(L \rightleftharpoons R)$, where $L \rightleftharpoons R$ represents the interchange between R and L. We see that, in the absence of electron-phonon scattering, Eq. (10) recovers the elastic Seebeck coefficient described in Ref. 28.

We now apply our theory to investigating the inelastic Seebeck effects of four Al atoms bridging the bimetallic Al electrodes modeled as electron jellium with $r_s \approx 2$. The 4-Al junction is structurally and electronically simple such that the first-principle calculations reported here can be performed with a high level of accuracy. It therefore serves as an ideal test bed for comparing the predictions of theory and measurements in experiments. We compare the elastic and inelastic Seebeck coefficients assuming that the left and right electrodes share the same temperature T_e. In order to qualitatively show to what extent local heating affects the inelastic Seebeck coefficient, we choose to display inelastic Seebeck coefficients with and without local heating.

In the case of "without local heating," we mean that the heat generated in the wire region is perfectly dissipated to electrodes such that $T_w = T_e$. When including "local heating," the effective local wire temperature T_w is higher than the electrode temperature T_e. Figure 2(a) shows T_w as a function of the applied bias V_B for various T_e. We note that three jumps occur at $V_B = 2.5$, 20, and 40 mV, corresponding to the energies of the normal modes. The sharp increase in T_w at $V_B = 20$ mV corresponds to the first longitudinal vibrational mode. Two degenerate transverse modes are present in the x and y directions at $V_B = 2.5$ mV, and we show the representative one in Fig. 2. Due to the selection rule, the contributions to local heating from modes with vibrational components perpendicular to the direction of electron transport (z direction) are unimportant. For $T_e = 0$, 4, and 10 K, T_w displays larger jumps at $V_B = 20$ mV, where eV_B is the energy of the first longitudinal vibrational mode. For $T_e = 50$ K, the signatures of normal modes in T_w are wiped out by high temperatures. The increase in local temperature is less significant at higher T_e. This is due to increasingly efficient heat dissipation caused by the increase of phonon population in the electrodes, as shown in Eq. (8). Figure 2(b) shows the inelastic profile of the conductance ($G = dI/dV$) and derivative of conductance (d^2I/dV^2) as a function of bias with and without local heating. Local heating enhances the effects of the electron-vibration interactions on the inelastic current because of increased average number of local phonons.

Figure 3(a) shows Seebeck coefficients as a function of the applied bias V_B for various T_e. For each temperature, we calculate Seebeck coefficients in three cases: elastic Seebeck coefficients S_0, inelastic Seebeck coefficients without local

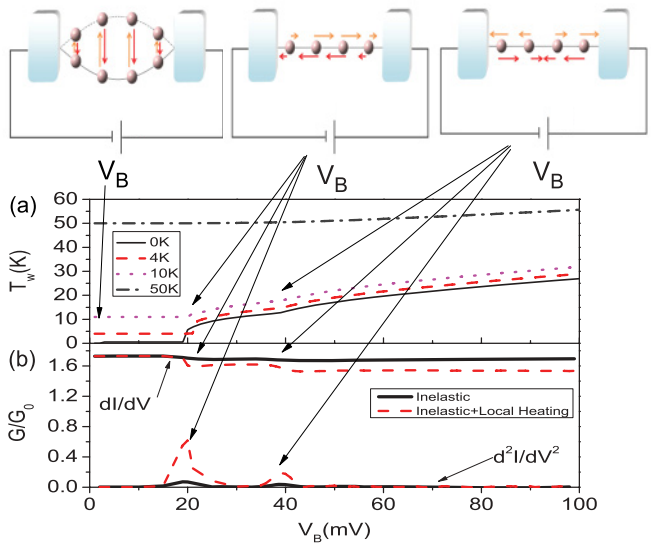

FIG. 2. (Color online) (a) Local temperature T_w as a function of V_B for $T_e = 0$, 4, 10, 50 K. (b) The differential conductance and the absolute value of dG/dV due the electron-vibration interaction without [solid (black) line] and with [dashed (red) line] local heating as a function of bias for $T_e = 12$ K. The schematic shows the normal modes that contribute to the jumps in the local temperature and inelastic current profiles.

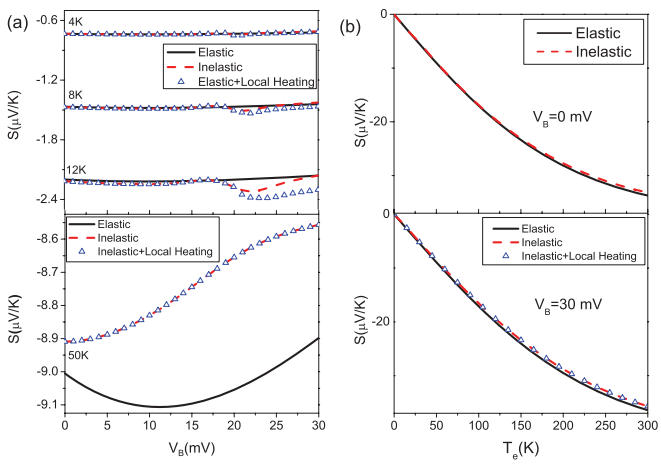

FIG. 3. (Color online) Elastic Seebeck coefficient [solid (black) line], inelastic Seebeck coefficient without local heating [dashed (red) line], and that with local heating [triangle (blue) line] (a) as a function of bias V_B for $T_e = 4$, 8, 12 K (top panel) and $T_e = 50$ K (bottom panel); and (b) as a function of T_e for $V_B = 0$ K (top panel) and and $V_B = 30$ K (bottom panel.)

heating S_1, and inelastic Seebeck coefficients with local heating S_2. The difference between the elastic and inelastic Seebeck effects is more salient in the low-temperature regime around $V_B = 20$ mV [see the cases of 4, 8, and 12 K in the top panel of Fig. 3(a)]. The profile of inelastic Seebeck coefficients vs V_B displays a strong signature corresponding to the longitudinal vibrational mode at $V_B = 20$ mV, where the magnitude of the Seebeck coefficients are increased. This feature is related to the suppression of the inelastic current around $V_B = 20$ mV, [Fig. 2(b)] where the transmission function effectively decreases. This leads to larger magnitudes of Seebeck coefficients because $S \propto -\tau'(\mu)/\tau(\mu)$.[28]

The inclusion of local heating enhances the effect of electron-vibration on Seebeck coefficients further. In the low-temperature regime, the top panel of Fig. 3(a) shows that S_1 (without local heating) significantly differs from S_2 (with local heating). This is because of the large difference between T_w and T_e, as shown in Fig. 2(a). For $V_B < 30$ mV, T_w and T_e become almost identical when the T_e is large. Consequently, the difference between S_1 and S_2 becomes small [see cases of $T_e = 50$ K in the lower panel of Fig. 3(a)]. In all cases, the transverse modes are negligible to the inelastic Seebeck coefficients. Figure 3(b) shows Seebeck coefficients as a function of T_e for $V_B = 0$ and 30 mV in three cases: S_0, S_1, and S_2. In the high-temperature regime ($T_e > 50$ K), the magnitudes of inelastic Seebeck coefficients (S_1 and S_2) are slightly decreased compared with the elastic Seebeck coefficients (S_0) due to small probability of electron-vibration scattering.

In summary, we investigated the elastic and inelastic Seebeck coefficients with and without local heating in the 4-Al atomic junction using first-principles calculations. In the low-temperature regime, the signature of normal modes in the profiles of inelastic Seebeck effects is salient. The inelastic Seebeck effects are enhanced by electron-vibration interactions due to the drastic suppression of the inelastic current at the bias corresponding to the normal mode with longitudinal vibrational character. Local heating enhances the inelastic Seebeck effects further due to increased average number of local phonons. In the high-temperature regime, the inelastic Seebeck effects are slightly suppressed by electron-vibration interactions due to quasiballistic electron transport in nanojunctions. The signature of normal modes in inelastic Seebeck coefficients and local temperatures is wiped out by the tail of the Fermi-Dirac distribution.

The authors thank the Ministry of Education Aim at Top University Plan (MOE ATU), the National Center for Theoretical Sciences (South) in Taiwan, and the National Science Council (Taiwan) for support (Grant No. NSC97-2112-M-009-011-MY3). Y.S. is thankful for the support of the NSFC (Grant No. 10947130).

*yuchangchen@mail.nctu.edu.tw

[1] M. Galperin, M. A. Ratner, and A. Nitzan, J. Phys. Condens. Matter **19**, 103201 (2007).
[2] L. H. Yu, C. D. Zangmeister, and J. G. Kushmerick, Phys. Rev. Lett. **98**, 206803 (2007).
[3] Y. C. Chen, Phys. Rev. B **78**, 233310 (2008).
[4] M. Kiguchi, O. Tal, S. Wohlthat, F. Pauly, M. Krieger, D. Djukic, J. C. Cuevas, and J. M. van Ruitenbeek, Phys. Rev. Lett. **101**, 046801 (2008).
[5] Y. C. Chen, M. Zwolak, and M. Di Ventra, Nano Lett. **3**, 1691 (2003); **4**, 1709 (2004); **5**, 621 (2005).
[6] T. Frederiksen, M. Brandbyge, N. Lorente, and A.-P. Jauho, Phys. Rev. Lett. **93**, 256601 (2004).
[7] Z. Huang, B. Xu, Y. C. Chen, M. Di Ventra, and N. J. Tao, Nano Lett. **6**, 1240 (2006).
[8] B. Ludoph and J. M. van Ruitenbeek, Phys. Rev. B **59**, 12290 (1999).
[9] P. Reddy, S. Y. Jang, R. A. Segalman, and A. Majumdar, Science **315**, 1568 (2007).
[10] Y. S. Liu, H. T. Yao, and Y. C. Chen, e-print arXiv:1001.0822v4; Y. S. Liu, B. C. Hsu, and Y. C. Chen, e-print arXiv:0908.0992v6.
[11] M. Paulsson and S. Datta, Phys. Rev. B **67**, 241403(R) (2003).
[12] X. Zheng, W. Zheng, Y. Wei, Z. Zeng, and J. Wang, J. Chem. Phys. **121**, 8537 (2004).
[13] F. Pauly, J. K. Viljas, and J. C. Cuevas, Phys. Rev. B **78**, 035315 (2008).
[14] Y. Dubi and M. Di Ventra, Nano Lett. **9**, 97 (2009).
[15] S. H. Ke, W. Yang, S. Curtarolo, and H. U. Baranger, Nano Lett. **9**, 1011 (2009).
[16] C. M. Finch, V. M. García-Suárez, and C. J. Lambert, Phys. Rev. B **79**, 033405 (2009).
[17] J. P. Bergfield and C. A. Stafford, Nano Lett. **9**, 3072 (2009).
[18] Y. S. Liu, Y. R. Chen, and Y. C. Chen, ACS Nano **3**, 3497 (2009).
[19] M. Galperin, K. Saito, A. V. Balatsky, and A. Nitzan, Phys. Rev. B **80**, 115427 (2009).
[20] T. Markussen, A. P. Jauho, and M. Brandbyge, Phys. Rev. B **79**, 035415 (2009).
[21] M. Galperin, A. Nitzan, and M. A. Ratner, Mol. Phys. **106**, 397 (2008).
[22] O. Entin-Wohlman, Y. Imry, and A. Aharony, Phys. Rev. B **82**, 115314 (2010).
[23] M. Esposito, K. Lindenberg, and C. V. den Broeck, Phys. Rev. Lett. **102**, 130602 (2009).
[24] N. D. Lang, Phys. Rev. B **52**, 5335 (1995).
[25] K. R. Patton and M. R. Geller, Phys. Rev. B **64**, 155320 (2001).
[26] Z. Yang, M. Chshiev, M. Zwolak, Y. C. Chen, and M. Di Ventra, Phys. Rev. B **71**, 041402(R) (2005).
[27] E. V. Chulkov and I. Yu. Sklyadneva, Surf. Sci. **331**, 1414 (1995).
[28] Y. S. Liu and Y. C. Chen, Phys. Rev. B **79**, 193101 (2009).